Designing Non-Periodic 3D Woven Composite Preforms Using LSTM Deep Learning Networks

Shemuel Joash Kuehsamy[1†][0009-0006-8958-1762], Haoran Zhou[1†], Zhen-Pei Wang[1*][0000-0002-5604-5940], David William Rosen[1,2][0000-0002-7257-9395]

[1] Institute of High Performance Computing (IHPC), Agency for Science, Technology and Research (A*STAR), 1 Fusionopolis Way, \#16-16 Connexis, Singapore 138632
[2]Singapore Institute of Manufacturing Technology (SIMTech), Agency for Science, Technology and Research (A*STAR), 5 Cleantech Loop #01-01 Singapore 636732

wangzp@ihpc.a-star.edu.sg

Abstract. Advanced 3D woven composites show significant promise for use in high-performance applications. Nonetheless, automating the design process for customized non-periodic woven architectures presents challenges due to the complexities arising from large-scale combinatorial design issues. This often leads to inefficient utilization of the tow reinforcement. In this work, by treating the woven design problem as a multi-agent system, we leverage an integrated framework combining the Hungarian Algorithm and Long Short-Term Memory (LSTM) networks. This allows for effective alignment of woven tows along loading paths, while enabling considerations of through-thickness reinforcement.

Keywords: 3D Woven Composites, Structural Design, Hungarian Algorithm, Long Short-Term Memory, Machine Learning, Multi-Agent System.

1 Introduction

3D woven composites were introduced for aerospace applications by NASA in the 1980s[1]. Since then, significant advancements in analysis, design, manufacturing, and testing have been achieved [2-18]. The use of 3D woven composites has expanded into sectors like automotive, sports equipment, medical implants, body armor, civil engineering, and prosthetics [19-25]. Particularly in aerospace, Ceramic Matrix Composites (CMC) are favored for advanced structures such as jet engines, spacecraft, and fusion reactors [26-28].

The 3D woven composites' structure, with its tow arrangements reducing delamination and enhancing impact tolerance, is crucial for aerospace applications against bird strikes [29]. Despite the potential of achieving near-net shapes through non-periodic integral woven designs [30-33], conventional designs often rely on

† Equal contribution

periodic weave patterns, leading to tow discontinuities caused by post machining process and limitations in overall structural performances.

Fully periodic designs can result in diminished mechanical performance due to machining-induced tow discontinuities and suboptimal tow alignment with load paths, limiting structural efficiency. Bio-inspired designs, like those of the human proximal femur [35], demonstrate the potential for optimized structures through strategic reinforcement arrangement [36].

Designing 3D tow architecture involves a combinatorial optimization problem at each intersection point, traditionally addressed through heuristic algorithms like the genetic algorithm or by comparing various designs to meet specific requirements [37-42]. Techniques for tow topology optimization and geometric design strategies aim to simplify design complexity at the micro-scale [43, 34, 44-48]. However, these methods are mostly applicable to periodic and micro-scale designs.

For integral designs of 3D woven composites with enhanced performance, strategic positioning of fibre tows is essential. Current designs, often based on knowledge-based approaches, are costly and inefficient, limiting customization and broader adoption of 3D woven composites [30-33, 49]. Although research using a homogenization approach is possible [50,51], it may pose continuity issues when incorporating heterogeneous units. The challenge of developing a concurrent design methodology for 3D woven composites remains unresolved after decades.

Building upon the advancements in the Background Vector Method (BVM) [52, 53], which facilitates concurrent creation of non-periodic 3D woven architectures at various scales, this study aims to establish a design methodology that combines the Hungarian Algorithm and Long Short-Term Memory (LSTM) networks. This approach is designed for the efficient and precise alignment of woven tows with the paths of applied loads, while preserving the other reinforcing considerations.

2 3D woven preform fabrication

We focus on 3D woven composite preforms that can be fabricated using Jacquard looms, as illustrated in Fig. 1. Such preforms typically consist of two groups of fibre tows that are orthogonal to each other. In Fig. 1, the warp tows are defined as parallel to the x-axis while the weft tows are the ones which are defined as parallel to the y-axis. The warp tows are grouped into stacks with the tows which share the same y-z plane being in the same stack. Similarly, for the weft tows, the tows which share the same x-z plane are grouped together in the same stack. The spacing between each warp stack in the y-direction is defined as δ_{warp} while the spacing between the weft stacks in the x-direction is defined as δ_{weft}.

The weaving process is as such, the weft tows are woven through each successive warp stack; the architecture of the preform depends on the position at which the weft tow passes through the warp stack. The orthogonal loom controls the position at which weft tow passes through the warp stack by raising or lowering the heddles according to the design. Thus, the design of the preform architecture can be broken down into topological ordering rules that dictate the positional arrangement of the warp and weft tows at any intersection.

The topological ordering used in this study aims to imitate the weaving process thus, at each intersection between a warp stack and weft stack, each weft tow in the stack is given an ordering integer,

$$\zeta_{j,q}^{(i)} = p \tag{1}$$

which determines that at the intersection of warp stack *i* and weft stack *j*, when the loom passes the *q*th weft tow through the intersection there are *p* warp tows below the weft tow, as illustrated in Tab. 1. Cases with multiple tows placed at the same location can be dealt with secondary ordering rules [31].

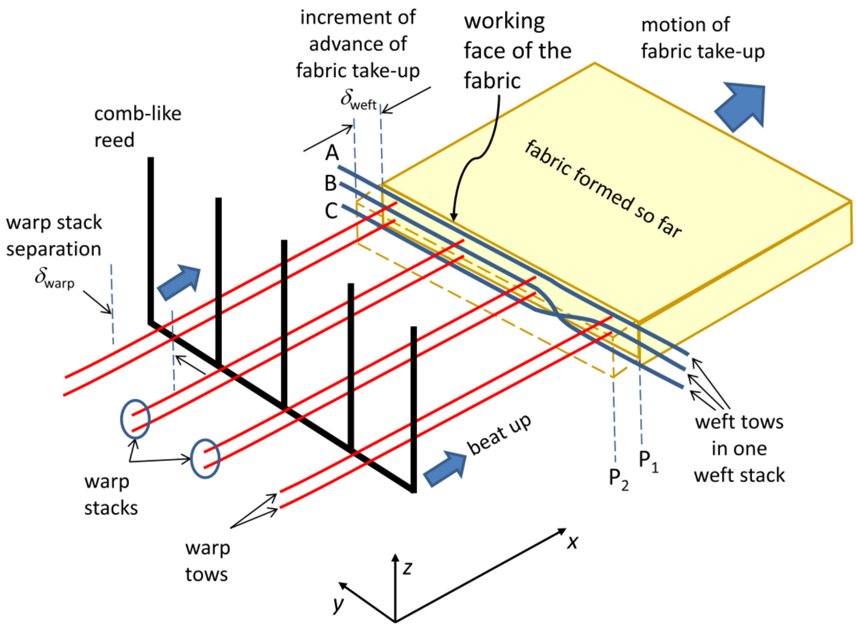

Fig. 1 Schematic of an orthogonal loom used to manufacture 3D woven composites [31].

Tab. 1 The locations of the weft tows *q* in weft stack *j* at intersections with different warp stacks *i* as specified by topological ordering rules [31].

	Weft tow *j,q*	Weft tow location							
		j,1	*j,2*	*j,3*	*j,4*	*j,5*	*j,6*	*j,7*	...
Warp stack *i*	1	$\zeta_{j,1}^{(i)}$	$\zeta_{j,2}^{(i)}$	$\zeta_{j,3}^{(i)}$	$\zeta_{j,4}^{(i)}$	$\zeta_{j,5}^{(i)}$	$\zeta_{j,6}^{(i)}$	$\zeta_{j,7}^{(i)}$	...
	2	$\zeta_{j,1}^{(i)}$	$\zeta_{j,2}^{(i)}$	$\zeta_{j,3}^{(i)}$	$\zeta_{j,4}^{(i)}$	$\zeta_{j,5}^{(i)}$	$\zeta_{j,6}^{(i)}$	$\zeta_{j,7}^{(i)}$	...
	...	...	...	...	...	...	...	...	...

3 Design method

This research introduces a method for designing non-periodic 2D sections by integrating the Hungarian Algorithm with a Long Short-Term Memory (LSTM) network. The core concept revolves around treating each tow as an agent at the starting stack, aiming for a position in the subsequent stack that maximizes its score. The Hungarian algorithm optimizes tow path placement in alignment with principal stress vectors to ensure the highest collective score among all agents. Meanwhile, the LSTM network incorporates elements of "human" experience into the design process.

3.1 Principal Stress Vectors

To align the tows with the component's loading paths, principal stress vectors are derived from the Finite Element Method (FEM) simulations. The resulting load path is an approximation, as the simulation employs a homogenized medium for simplification. An illustrative example provided in Fig. 2 depicts a three-point bending problem spanning a 120x20 domain, with a free roller support at three-quarters of its length and a point load of 500N. The material is characterized by a Poisson's ratio of 0.3 and a Young's Modulus of 70 GPa. Warp tows, represented by circles, extend out-of-plane. Von Mises stress distribution contours, generated through iso-geometric analysis on a 50 x 10 mesh, illustrate the stress patterns. Load path vectors are delineated along the central line between two warp tow stacks (visualized as column of circles in Fig. 2). At each specified point within the 2D domain, two principal stress vectors are identified, collectively forming a set of vectors.

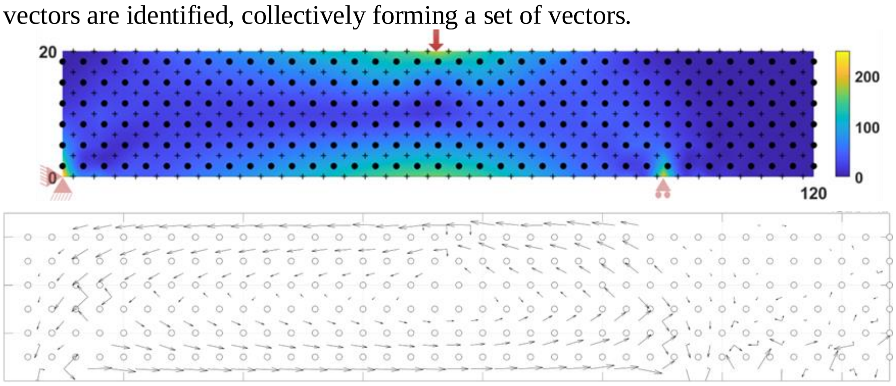

Fig. 2 The Von Mises stress distributions in a beam in asymmetric three-point bending, with normalized principal stress vector fields. Load and supports as indicated. Black circles indicate the positions of warp tows for textile design, aligned vertically [52].

3.2 Tow Path Vectors

Tow path vectors refers to the path taken by a tow between two consecutive warp stacks. The location of the weft tow at each intersection is interpreted as the number of warp tows below the weft tows. For the ith weft tow located at φ_i^o at the current warp stack o and φ_i^{o+1} at the next warp stack $o+1$, the corresponding normalized vector for the tow path is:

$$\boldsymbol{v}_{(i,o)} = \frac{1}{\|[\delta w, \varphi_i^{o+1} - \varphi_i^o]\|} [\delta w, \varphi_i^{o+1} - \varphi_i^o]^{\mathrm{T}} \quad (2)$$

where δw is the width between two neighbouring warp tow stacks.

Particularly, for the weft tow locations interpreted as the number of warp tows with the same type and size beneath it, the tow path vector can be simplified as

$$\boldsymbol{v}_{l(i,o)\to k} = \frac{1}{\|[\delta w, (k-l(i,o))\delta h]\|}\left[\delta w, \left(k - l(i,o)\right)\delta h\right] \tag{3}$$

where $l(i,o)$ is the current location of tow i in the current stack o, k is the position of the tow in the next warp stack $o+1$, and δh is the thickness of warp tows.

3.3 Hungarian Algorithm

The initial BVM developed in references [52,53] addresses a three-sided matching challenge involving three components: the starting tow location, the background vector, and the subsequent tow location. It is well known that a 3-matching problem is NP-hard [54], and the corresponding approximation problem is APX-complete [55]. To reduce the complexity of the matching game so that the well-established Hungarian algorithm [56] can be applied, we simplify the problem by rearranging the use of background vectors.

First, we only keep the largest background vector corresponding to the loading path at the location of the tow path's starting point, eliminating background vectors that facilitate other reinforcement considerations. Second, these additional reinforcement considerations are addressed by LSTM networks, acting as a human expert factor.

Consequently, the three-sided matching problem is transformed into a two-sided matching game between the tow's starting location, φ_i^o, and the next location, φ_i^{o+1}. This two-sided matching game can be solved using the Hungarian algorithm in a straightforward manner.

In other words, the Hungarian Algorithm [56] is utilized in this study to assign tow locations, specifically to place weft tows in the ith stack into positions in the $i+1$ stack. As illustrated in Fig. 3, the goal is to reassign weft tows currently in positions 1 to 5 to positions 6-10 in the next warp stack, thereby maximizing the tow's alignment with the principal stress directions. This scenario can be modeled as a bipartite graph with weighted edges that quantify the alignment, where the edge weights are given by:

$$w_{ik} = V_L^{i,j} \cdot \boldsymbol{v}_{l(i,o)\to k} \tag{4}$$

where i is the position of the weft tow in the current stack and k is the possible position of the weft tow in the next stack. The Hungarian algorithm is an efficient means of solving combinatorial optimization problems such as this assignment problem within a polynomial time complexity. Thus, using the Hungarian algorithm, an optimal matching with the maximum cost can be found, which maximizes the efficiency of the tow alignments. The Hungarian Algorithm will be employed to sequentially assign the tows to a location in each warp-weft stack intersection throughout the entire structure.

3.4 Long Short-Term Memory (LSTM) Network

Reducing the matching problem from three-sided to two-sided leads to the absence of considerations for other reinforcing requirements. One mechanism to ensure all reinforcement requirements are met at all intersections is to assign each weft tow a specific reinforcement task a priori. Such an approach is highly ad-hoc and often observed in 3D woven designs as binders or interlayer locking tows. We enable these tows to develop a nuanced preference using a neural network.

The Long Short-Term Memory Network [57,58], a type of Recurrent Neural Network, features feedback connections that allow the network to accumulate a long-term memory of a sequence of data points. It is commonly utilized for making predictions on time-series data; in this context, we apply it to take the location history of a tow in the preceding stacks to predict the location of the weft tow in the next stack.

The LSTM is employed to incorporate "human" knowledge into designs generated using the Hungarian algorithm through the following steps. Initially, this framework requires training different LSTM models with the location data of tows designated for specific functions. Then, selected tows are assigned a particular function, and their locations are predicted using the LSTM. Finally, the locations of the remaining tows are determined using the Hungarian algorithm.

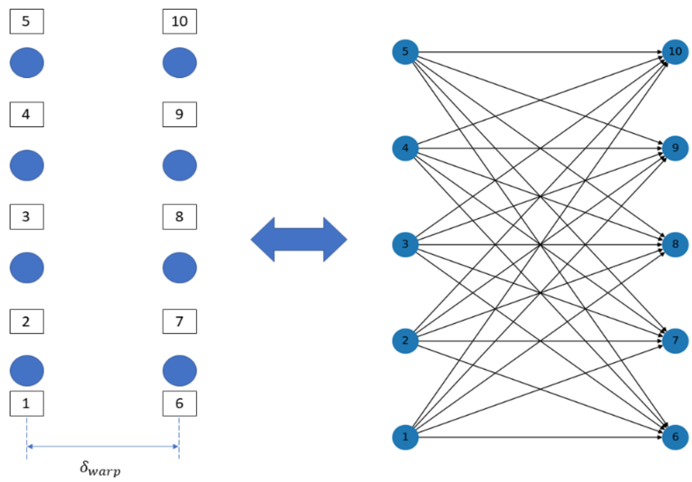

Fig. 3 Example of how an interval between two intersections can be modelled as a bipartite graph.

4 Results

To demonstrate the combined use of an LSTM and the Hungarian algorithm, we examine the case of a 2D simply supported bridge illustrated in Figure 2. The principal stress vectors, extracted from finite element simulations, are used to guide the direction of the tow paths. In the first design iteration, depicted in Figure 4, tow placement is solely managed by the Hungarian algorithm.

In contrast, the second iteration employs both the LSTM and the Hungarian algorithm, as shown in Figure 5. Two tow are selected to be used as binders. A LSTM is trained to achieve the tow functions. The LSTM network architecture is show in Table 2.

Table 2. LSTM network architecture.

Layer	Output
LSTM	32
Dense	9
Dense	12
Dense	4

The comparison between Figures 4 and 5 reveals that using only principal stress vectors leads to tow paths that are mostly straight in the middle section to combat bending, while the ends of the paths adopt more vertical directions. However, the integration of both the Hungarian Algorithm and LSTM results in a more varied tow path layout, with paths that feature a through-thickness orientation being more consistently implemented throughout the structure.

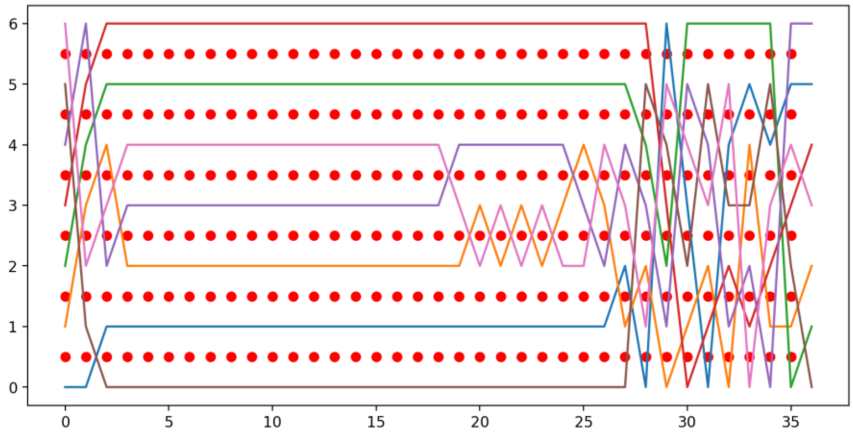

Fig. 4 Example of a design using only the Hungarian Algorithm.

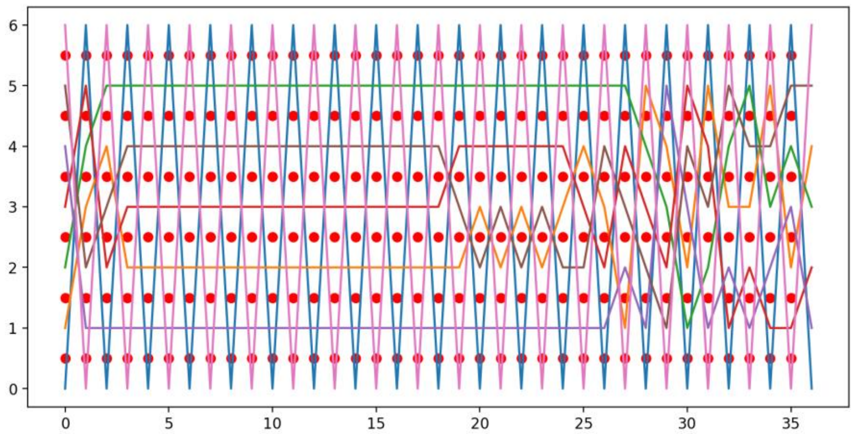

Fig. 5 Example of a design using both Hungarian algorithm and LSTM. Through-thickness reinforcement is clearly enhanced.

5 Conclusion

The design challenge of 3D woven architectures is addressed in this work by conceptualizing each tow as an agent aiming to maximize its individual score, with the Hungarian algorithm serving as the mechanism for attaining perfect matching. Additionally, the LSTM contributes “human experience,” bolstering the reinforcement potentially compromised in the transition from a three-sided matching to a two-sided matching. The approach proposed can accomplish tow alignment that is tailored for the specific loads it may face.

Acknowledgements

This research is supported by A*STAR $<C210112026>$ (Career Development Fund (CDF) – 2020) and D.W. Rosen's A*STAR start-up fund. The authors would like to thank Dr. Brian N. Cox, Dr. N. Sridhar, and Dr. Mark H. Jhon for the communications related to 3D woven composites.

References

1. H. B. Dexter, Development of textile reinforced composites for aircraft structures, 4th International Symposium for Textile Composites (1998).
2. J. Byun, T. Chou, Modelling and characterization of textile structural composites: A review, The Journal of Strain Analysis for Engineering Design 24 (1989) 253–262.
3. B. N. Cox, G. Flanagan, Handbook of analytical methods for textile composites (1997).
4. F. Desplentere, S. V. Lomov, D. Woerdeman, I. Verpoest, M. Wevers, A. Bogdanovich, Micro-ct characterization of variability in 3D textile architecture, Composites Science and Technology 65 (2005) 1920–1930.
5. A. C. Long, Design and manufacture of textile composites, Elsevier, 2005.
6. X. Chen, Modelling and predicting textile behaviour, Elsevier, 2009.
7. M. Ansar, W. Xinwei, Z. Chouwei, Modeling strategies of 3D woven composites: A review, Composite structures 93 (2011) 1947–1963.
8. X. Chen, L. W. Taylor, L.-J. Tsai, An overview on fabrication of three-dimensional woven textile preforms for composites, Textile Research Journal 81 (2011) 932–944.17
9. K. Bilisik, Multiaxis three-dimensional weaving for composites: a review, Textile Research Journal 82 (2012) 725–743.
10. T. Gereke, O. Dobrich, M. Hubner, C. Cherif, Experimental and computational composite textile reinforcement forming: A review, Composites Part A: Applied Science and Manufacturing 46 (2013) 1–10.
11. Liu, Y., Hou, Y., Sapanathan, T., Meng, L., & Xu, Y. (2023). Multiscale modeling of the mechanical behavior of 3D braided CFRP composites under uniaxial tension. Composite Structures, 306, 116601.
12. V. Carvelli, S. V. Lomov, Fatigue damage evolution in 3D textile composites, in: Fatigue of textile composites, Elsevier, 2015, pp. 223–253.
13. X. Chen, L. Chen, C. Zhang, L. Song, D. Zhang, Three-dimensional needle-punching for composites–a review, Composites Part A: Applied science and manufacturing 85 (2016) 12–30.

14. H. M. El-Dessouky, M. N. Saleh, 3D woven composites: from weaving to manufacturing, Recent Developments in the Field of Carbon Fibers 51 (2018).
15. Y. E. Elmogahzy, Engineering textiles: Integrating the design and manufacture of textile products, Woodhead Publishing, 2019.
16. M. Mehdikhani, L. Gorbatikh, I. Verpoest, S. V. Lomov, Voids in fiber-reinforced polymer composites: A review on their formation, characteristics, and effects on mechanical performance, Journal of Composite Materials 53 (2019) 1579–1669.
17. M. Bodaghi, S. Lomov, P. Simacek, N. Correia, S. Advani, On the variability of permeability induced by reinforcement distortions and dual scale flow in liquid composite moulding: A review, Composites Part A: Applied Science and Manufacturing 120 (2019) 188–210.
18. T. Gereke, C. Cherif, A review of numerical models for 3D woven composite reinforcements, Composite Structures 209 (2019) 60–66.
19. A. P. Mouritz, M. K. Bannister, P. Falzon, K. Leong, Review of applications for advanced three-dimensional fibre textile composites, Composites Part A: applied science and manufacturing 30 (1999) 1445–1461.
20. N. Naik, P. Shrirao, Composite structures under ballistic impact, Composite structures 66 (2004) 579–590.
21. N. M. Aly, A review on utilization of textile composites in transportation towards sustainability, in: IOP conference series: materials science and engineering, volume 254, IOP Publishing, 2017, p. 042002.
22. N. S. Karaduman, Y. Karaduman, H. Ozdemir, G. Ozdemir, Textile reinforced structural composites for advanced applications, Textiles for advanced applications (2017) 87.
23. T. Huang, Y. Wang, G. Wang, Review of the mechanical properties of a 3D woven composite and its applications, Polymer-Plastics Technology and Engineering 57 (2018) 740–756.
24. A. Saboktakin, 3D textile preforms and composites for aircraft strcutures: A review, International Journal of Aviation, Aeronautics, and Aerospace 6 (2019) 2.
25. L. Limmer, G. Weissenbach, D. Brown, R. McIlhagger, E. Wallace, The potential of 3-d woven composites exemplified in a composite component for a lower-leg prosthesis, Composites Part A: Applied Science and Manufacturing 27 (1996) 271–277.
26. H. Ohnabe, S. Masaki, M. Onozuka, K. Miyahara, T. Sasa, Potential application of ceramic matrix composites to aero-engine components, Composites Part A: Applied Science and Manufacturing 30 (1999) 489–496.
27. W. Krenkel, Ceramic matrix composites: fiber reinforced ceramics and their applications, John Wiley & Sons, 2008.
28. K. K. Chawla, Ceramic matrix composites, Springer Science & Business Media, 2013.
29. B. Behera, , B. Dash, Mechanical behavior of 3D woven composites, Materials & design 67 (2015) 261–271.
30. B. Cox, Q. Yang, D. Marshall, J. Davis, Design issues in using integral textile ceramic composites in turbine engine combustors, Journal of propulsion and power 21 (2005) 314–326.
31. B. N. Cox, G. Nilakantan, O. Sudre, D. B. Marshall, Generating virtual specimens for complex non-periodic woven structures by converting machine instructions into topological ordering rules, Composite Structures 141 (2016) 63–78.
32. D. B. Marshall, B. N. Cox, Integral textile ceramic structures, Annual Review of Materials Research 38 (2008) 425443.
33. D. B. Marshall, B. N. Cox, O. H. Sudre, Integral textile structure for 3D CMC turbine airfoils, 2017. US Patent 9,664,053.

34. [34] J. Quinn, R. McIlhagger, A. McIlhagger, A modified system for design and analysis of 3D woven preforms, Composites Part A: applied science and manufacturing 34 (2003) 503–509.
35. C. Boyle, I. Y. Kim, Three-dimensional micro-level computational study of wolff's law via trabecular bone remodeling in the human proximal femur using design space topology optimization, Journal of biomechanics 44 (2011) 935–942.
36. Wang, J., Westermann, R., & Wu, J. (2023). A streamline-guided dehomogenization approach for structural design. Journal of Mechanical Design, 145(2), 021702.
37. S. J. Kuehsamy, Z.-P. Wang, M. J. Jhon, F. Yang, N. Sridhar, Design optimization of integral stiffeners for 3D woven composite preforms, Structures (2024), in press.
38. A. A. Pelegri, D. N. Kedlaya, Design of composites using a generic unit cell model coupled with a hybrid genetic algorithm, Composites Part A: Applied Science and Manufacturing 39 (2008) 1433–1443.
39. X. Zeng, A. C. Long, I. Ashcroft, P. Potluri, Fibre architecture design of 3D woven composite with genetic algorithms: a unit cell based optimisation framework and performance assessment, 20th International Conference on Composite Materials, Copenhagen, 19-24th July (2015).
40. X. Fu, S. Ricci, C. Bisagni, Minimum-weight design for three dimensional woven composite stiffened panels using neural networks and genetic algorithms, Composite structures 134 (2015) 708–715.
41. Q. Wang, X. Yang, H. Zhao, X. Zhang, G. Cao, M. Ren, Microscopic residual stresses analysis and multiobjective optimization for 3D woven composites, Composites Part A: Applied Science and Manufacturing 144 (2021) 106310.
42. D. Hartranft, A. Pravizi-Majidi, T.-W. Chou, Modeling and characterization of through-the-thickness properties of 3D woven composites, in: NASA, Langley Research Center Mechanics of Textile Composites Conference, 1995.
43. S. Ha, J. K. Guest, Topology optimization of 3D woven micro-lattices using a projection-based ground structure approach, in: 17th AIAA/ISSMO Multidisciplinary Analysis and Optimization Conference, 2016, p. 3214.
44. I. Verpoest, S. V. Lomov, Virtual textile composites software wisetex: Integration with micro-mechanical, permeability and structural analysis, Composites Science and Technology 65 (2005) 2563–2574.
45. H. Lin, L. P. Brown, A. C. Long, Modelling and simulating textile structures using texgen, in: Advanced Materials Research, volume 331, Trans Tech Publ, 2011, pp. 44–47.
46. A. R. Labanieh, X. Legrand, V. Koncar, D. Soulat, Novel optimization method to estimate the geometrical properties of a multiaxial 3D woven preform, Journal of Reinforced Plastics and Composites 32 (2013) 700–712.
47. G. Spackman, L. Brown, I. Jones, Development of methods for optimisation of complex 3D weave geometries, in: IOP Conference Series: Materials Science and Engineering, volume 406, IOP Publishing, 2018, p. 012029.
48. E. Plaka, S. Jones, B. A. Bednarcyk, E. J. Pineda, R. Li, M. Maiaru, Application of a rapid design tool to a 3D woven structural joint, in: AIAA SCITECH 2022 Forum, 2022, p. 1009.
49. S. Yan, X. Zeng, A. Long, Meso-scale modelling of 3D woven composite t-joints with weave variations, Composites Science and Technology 171 (2019) 171–179.
50. K. Morioka, Y. Ohtake, H. Suzuki, Y. Nagai, H. Hishida, K. Inagaki, T. Nakamura, F. Watanabe, 3D woven composite design using a flattening simulation, Computer-Aided Design 81 (2016) 24–38.

51. X. Fu, S. Ricci, C. Bisagni, Multi-scale analysis and optimisation of three-dimensional woven composite structures combining response surface method and genetic algorithms, CEAS Aeronautical Journal 8 (2017) 129–141.
52. Wang, Z. P., Cox, B. N., Kuehsamy, S. J., Jhon, M. H., Sudre, O., Sridhar, N., & Conduit, G. J. (2024). A compact yet flexible design space for large-scale nonperiodic 3D woven composites based on a weighted game for generating candidate tow architectures. Computer-Aided Design, 167, 103637.
53. Wang, Z. P., Kuehsamy, S. J., Rosen D. W. (2024). A Generalized Background Vector Method for Designing 3D Non-Periodic Woven Preforms Using Topological Orderings, under review.
54. Okura T. Materials for Aircraft Engines. ASEN 5063 Aircraft Propulsion Final Report, 2015.
55. I. Gnaba, X. Legrand, P. Wang, D. Soulat, Through-the-thickness reinforcement for composite structures: A review, Journal of industrial textiles 49 (2019) 71–96.
56. Karp, Richard M. Reducibility among Combinatorial Problems."Complexity of Computer Computations, 1972, 85–103.
57. Crescenzi, Pierluigi, Viggo Kann, Magnus Halldorsson, Marek Karpinski, and Gerhard Woeginger. Maximum 3-dimensional matching. A Compendium of NP Optimization Problems (2000).
58. Hochreiter, Sepp, and Jürgen Schmidhuber. Long short-term memory. Neural computation 9, no. 8 (1997): 1735-1780